



HAL
open science

3D genome alterations and editing in pathology

Eugenia Tiukacheva, Sergey Ulianov, Anna Karpukhina, Sergey Razin, Yegor Vassetzky

► **To cite this version:**

Eugenia Tiukacheva, Sergey Ulianov, Anna Karpukhina, Sergey Razin, Yegor Vassetzky. 3D genome alterations and editing in pathology. *Molecular Therapy*, 2023, 31 (4), pp.924-933. 10.1016/j.ymthe.2023.02.005 . hal-04230078

HAL Id: hal-04230078

<https://hal.science/hal-04230078>

Submitted on 5 Oct 2023

HAL is a multi-disciplinary open access archive for the deposit and dissemination of scientific research documents, whether they are published or not. The documents may come from teaching and research institutions in France or abroad, or from public or private research centers.

L'archive ouverte pluridisciplinaire **HAL**, est destinée au dépôt et à la diffusion de documents scientifiques de niveau recherche, publiés ou non, émanant des établissements d'enseignement et de recherche français ou étrangers, des laboratoires publics ou privés.

[Click here to view linked References](#)

1

2 **3D genome alterations and editing in pathology**

3

4 Eugenia Tiukacheva^{1,2}, Sergey Ulianov^{2,3} Anna Karpukhina^{1,4}, Sergey Razin^{2,3} and Yegor
5 Vassetzky^{1,4,5}

6 ¹CNRS UMR9018, Institut Gustave Roussy, Villejuif, France;

7 ²Institute of Gene Biology, Moscow, Russia;

8 ³Faculty of Biology, Lomonosov Moscow State University, Moscow, Russia;

9 ⁴Koltzov Institute of Developmental Biology, Moscow, Russia;

10 ⁵Corresponding author

11

12

13 Keywords: Genetic Diseases, Cancer, 3D genome, epigenome editing, therapy.

14

15 **Highlights**

- 16
- 17 • Genome is folded into a multi-level 3D structure that controls many nuclear functions,
including gene expression
 - 18 • Alterations in 3D genome organization are linked to genetic diseases and cancer
 - 19 • Several approaches have been developed to modify the global 3D genome
20 organization and that of specific loci.
 - 21 • Emerging experimental approaches of 3D genome editing may prove useful in
22 biomedicine

23 **Abbreviations**

24

25 ABA - abscisic acid

26 ADLD - autosomal-dominant adult-onset demyelinating leukodystrophy

27 adRP - autosomal-dominant retinitis pigmentosa

28 AML - acute myeloid leukemia

29 BOFS - branchiooculofacial syndrome

30 CBS - CTCF binding site

31 CLOuD9 - chromatin loop reorganization using CRISPR-dCas9

32 CNS - central nervous system

33 CT - chromosome territory

34 FSHD - facioscapulohumeral muscular dystrophy

35 LAD - lamina-associated domain

36 LADL - light-activated dynamic looping

37 LCR - locus control region

38 NAD - nucleolus-associated domain

39 STR - short tandem repeats

40 SV - structural variation

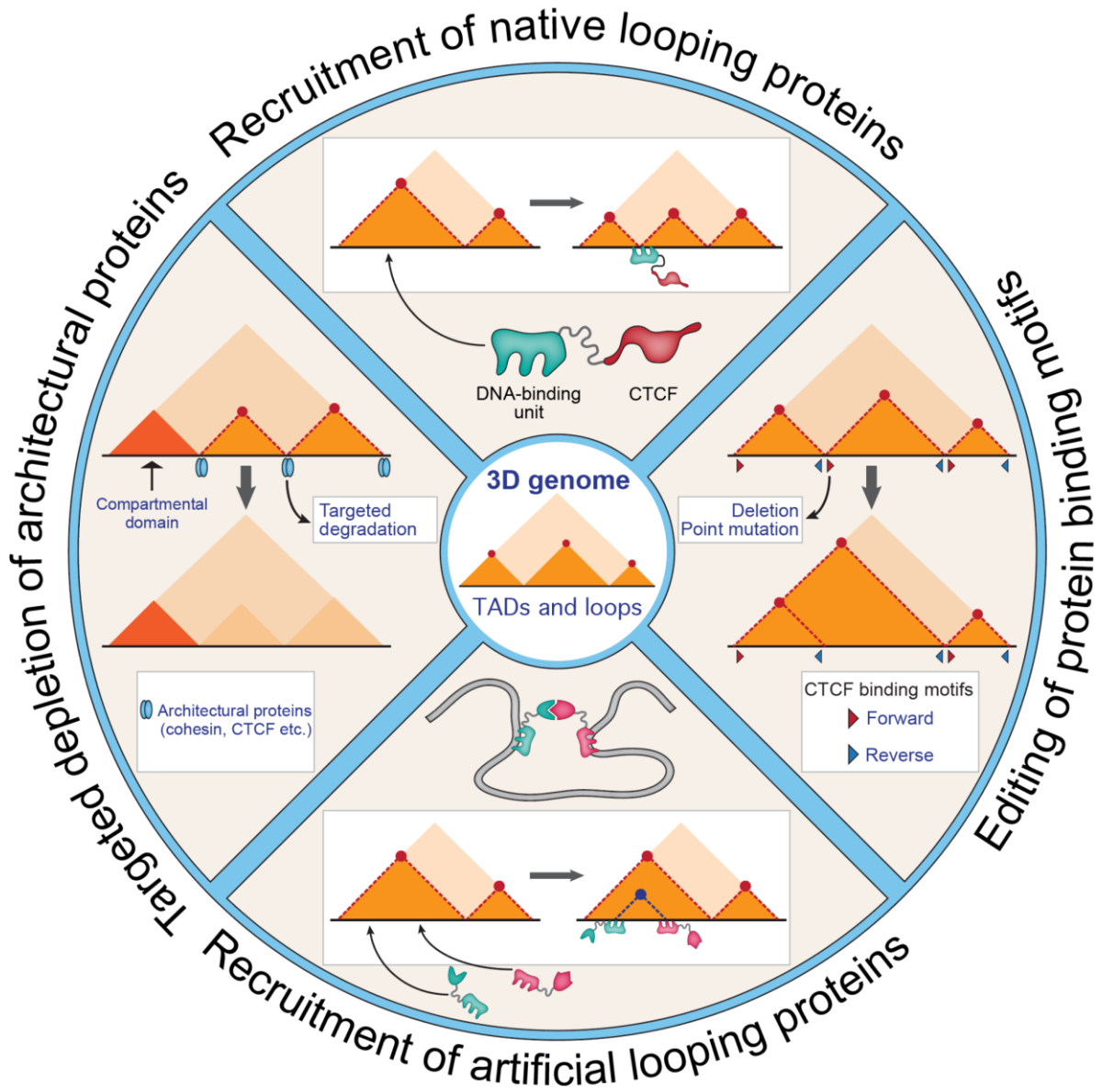
41 T-ALL - T-cell acute lymphoid leukemia

42 TAD - topologically associating domain

43 TALE - transcription activator-like effector

44 TF - transcription factor

45 ZFs - zinc finger nucleases



53 **ABSTRACT**

54 Human genome is folded into a multi-level 3D structure that controls many nuclear functions,
55 including gene expression. Recently, alterations in 3D genome organization were
56 associated with several genetic diseases and cancer. As a consequence, experimental
57 approaches are now developed to modify the global 3D genome organization and that of
58 specific loci. Here we discuss emerging experimental approaches of 3D genome editing that
59 may prove useful in biomedicine.

60

61 **The overall 3D genome organization**

62 The interphase genome is folded in a highly ordered manner, essential both for DNA
63 compaction and for the regulation of various intranuclear processes. Each chromosome
64 occupies a restricted volume in the nucleus, a chromosome territory (CT). In mammals, large
65 chromosomes and chromosomes with low gene density tend to localise at the nuclear
66 periphery, whereas smaller chromosomes with high gene density are located more centrally
67 (Boyle et al., 2001; Crosetto and Bienko, 2020). CTs have a spongy internal structure and
68 are composed of bulk chromatin masses penetrated with the channels of the “interchromatin
69 compartment”, a dynamically organized system of cavities serving for the diffusion of
70 nucleoplasm components (Albiez et al., 2006).

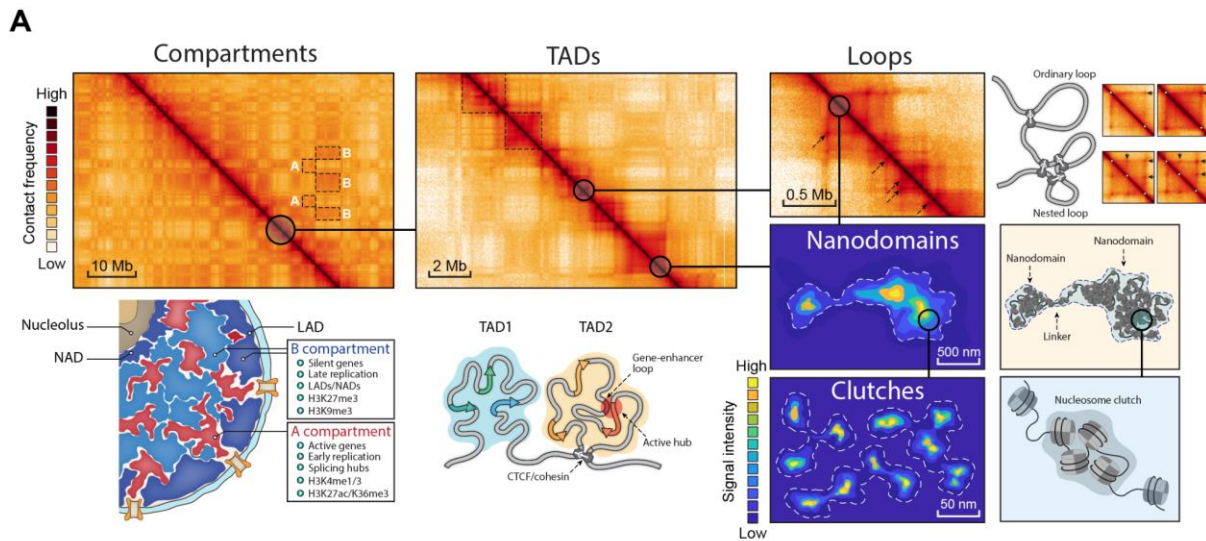
71

72 Within CTs, active and repressed genomic regions are spatially segregated into A and B
73 compartments, respectively, formed by local *cis* as well as distant *cis* and *trans* interactions
74 (Figure 1A) (Lieberman-Aiden et al., 2009). *A compartments* are early-replicating gene-rich
75 and typically highly transcribed regions enriched in active histone marks such as H3K36me3,
76 H3K27ac and H3K4me1. In contrast, *B compartments* contain late-replicating
77 transcriptionally silenced regions enriched with nucleolus- and lamina-associated domains
78 (NaDs and LADs, respectively) marked with H3K9me2 and H3K9me3 (Dillinger et al., 2017;
79 Guelen et al., 2008; Nichols and Corces, 2021; Rao et al., 2014). Compartment partitioning
80 strongly correlates with the transcription profile and thus is highly cell type-specific (Dixon et

81 al., 2015; Winick-Ng et al., 2021), whereas compartmentalization degree might vary
82 significantly within a cell population (Bintu et al., 2018; Kim et al., 2020).
83
84 The compartments are further divided into subcompartments, distinguished by the patterns
85 of different histone modifications and further into topologically-associated domains (TADs)
86 with a high CTCF/cohesin occupancy at their borders (Gómez-Marín et al., 2015;
87 Merckenschlager and Nora, 2016) and representing globular structures with a remarkable
88 cell-to-cell variability in their 3D shape and folding density (Stevens et al., 2017). TADs serve
89 as “warehouses” for genes, gene loci and their regulatory systems (Razin et al., 2016)
90 delimiting the areas of enhancer action (Nora et al., 2017). Consequently, genes within a
91 TAD are often co-regulated (Dixon et al., 2016); this is achieved by looping between
92 enhancers/locus control regions and promoters (Amândio et al., 2020; Bonev et al., 2017).
93 Molecular details of the loop formation mechanisms are still not fully understood, but
94 cohesin-driven extrusion (Bauer et al., 2021; Davidson et al., 2019) and liquid-liquid phase
95 separation (Hnisz et al., 2017; Razin and Gavrilov, 2020) are the most consistent models.
96 The CTCF-cohesin complex preferentially determines strong long-range interactions including
97 contacts between TAD borders (Rao et al., 2014), while the short-range enhancer-promoter and
98 promoter-promoter interactions are also maintained through Mediator complex and various
99 transcription factors (TFs) (Krietenstein et al., 2020) in cooperation with transcription machinery
100 (Hsieh et al., 2020). Complex contact patterns within TADs are manifested in non-structured
101 hierarchical nucleosome assemblies such as clutches (Ricci et al., 2015) and nanodomains
102 (Szabo et al., 2018). Clutches are relatively small nucleosome agglomerates (about 2-20
103 nucleosomes/clutch) whose density and size strongly depend on the level of histone
104 acetylation. This implies that clutches are formed by weak transient electrostatic interactions
105 between nucleosomes. A group of clutches constitutes a nanodomain. Nanodomains are
106 distributed throughout the nucleus, but their concentration increases near the nuclear
107 periphery. Nanodomain structures are preserved upon CTCF and cohesin degradation and

108 they seem to be formed through liquid-liquid phase separation (Szabo et al., 2020; Ulianov
 109 et al., 2021).

110



B

Structure	Size and assay	Putative functions	Editing strategy
Identified by C-methods			
Compartments	0.5-10 Mb, Hi-C	Spatial segregation of active and inactive chromatin	Unknown
TADs	0.1-1 Mb, Hi-C, 5C	Spatial insulation of neighboring genome loci and their regulatory systems	Mutations and rearrangements of CBSs
Loops	50-500 kb, Hi-C, 4C, Capture-C	Spatial insulation of neighboring genome loci and contacts between regulatory regions	Same as for TADs + CTCF recruitment
Identified by microscopy			
Nanodomains	0.007-0.2 mkm ² , Oligopaint-FISH	Unknown	Unknown
Clutches	100-1000 nm ² , ICH, Chrom-EMT	Unknown	Unknown

111

112 **Figure 1.** Different levels of 3D genome organization. A, Upper panel: contact maps of 3D
 113 genome structures, lower panel: graphical representation; B, summary of different levels of
 114 3D genome organization.

115

116 In sum, TADs represent cornerstone structural and functional units of the 3D genome. Below
 117 we highlight the role of TAD rearrangement and disruption of TAD borders in the
 118 development of severe pathologies, and discuss 3D genome editing techniques..

119

120 **3D organization of the genome and pathologies**

121

122 Over several past years, a number of pathologies have been associated with 3D genome
123 structure abnormalities. Changes in loop and TAD profiles can be due to both genetic and
124 epigenetic factors. The most common are SV (structural variation) mutations:
125 rearrangements of 50 nucleotides or more in length such as deletions, duplications,
126 insertions and translocations. SV mutations affecting the 3D genome in various diseases
127 modulate promoter-enhancer interactions and affect gene expression (Nieboer and de
128 Ridder, 2020; Zhang et al., 2021). They can change the proximity or accessibility of affected
129 genomic regions, increasing the risks for certain chromosomal aberrations (Yang et al.,
130 2022).

131

132 CTCF binding sites (CBSs) serve as barriers for cohesin-driven DNA-loop extrusion, the
133 major determinant of a TAD profile in mammals (Nuebler et al., 2018). DNA methylation
134 suppresses CTCF binding; thus allowing aberrant enhancer-promoter interactions that may
135 affect disease-related genes. As we discuss below, this effect is common to several human
136 diseases

137

138 In human glioma, mutations in the *IDH* gene result in an increased genome-wide level of
139 DNA methylation including that in the *PDGFRA* oncogene locus. Methylation of the 5'-
140 flanking insulator serving as a TAD boundary in this locus results in loss of CTCF binding
141 and perturbs local interaction patterns that drives an abnormal activation of the *PDGFRA*
142 gene by a distal enhancer (Flavahan et al., 2016).

143 In human 3p21.2 locus, the SV rs2535629 have a strong association with schizophrenia.
144 rs2535629 (A/G) is located within the CBS which resides in a repressor element in the 7th
145 intron of the *ITIH3* gene. The presence of this structural variation prevents CTCF binding to
146 CBS, and also changes the expression profiles of nearby genes: downregulates *GLT8D1*
147 and *SFMBT1*, and upregulates *NEK4*. Downregulation of *SFMBT1* gene product involved in
148 the regulation of proliferation and differentiation of nerve stem cells, as well as in the

149 formation of dendritic spines and the proper functioning of neural synapse, is associated with
150 schizophrenia development (Li et al., 2022).

151 SVs within enhancers interacting with *MYH7* and *LMNA* can trigger the development of
152 cardiomyopathy. *MYH7* and *LMNA* promoters establish spatial contacts with multiple
153 enhancers, sometimes in a clustered manner. Many of these enhancers contain binding
154 sites of various TFs including CTCF. Several SNPs (rs7149564, rs116554832 or
155 rs10873105) suppress TF binding to DNA, probably affecting enhancer-promoter loops. For
156 example, the SNP rs875908, 2 kb away from *MYH7*, destroys the TBX5 binding motif and is
157 associated with a decrease in the thickness of the left ventricle in dilated cardiomyopathy
158 (Gacita et al., 2021).

159 A myopathy associated with a SV affecting CBS is facioscapulohumeral muscular dystrophy
160 (FSHD). This disease is related to the abnormal expression of the *DUX4* gene and other
161 genes, such as *FRG1* and *FRG2*, have been proposed to contribute to FSHD pathology.
162 Enhancers regulating *DUX4* and *FRG1* and their target genes are physically separated into
163 two different loops due to the presence of an FR-MAR insulator (Himeda et al., 2014; Petrov
164 et al., 2006, 2008). The insulator activity of FR-MAR is decreased by the presence of a
165 certain SSLP and specific CpG methylation within the region in FSHD myoblasts (Kisseljova
166 et al., 2014; Petrov et al., 2008).

167 In T-cell acute lymphoid leukaemia (T-ALL), multiple changes in gene activity and the profile
168 of CTCF binding to DNA coincide within specific TADs, with a major impact on
169 carcinogenesis-related regions in *NOTCH1* target genes (such as *APCDD1*, *IKZF2*, *CYLD*
170 and *MYC* (Kloetgen et al., 2020). Disappearance of the TAD boundary between *MYC* and its
171 superenhancer in T-ALL cells leads to Myc overexpression (Kloetgen et al., 2020). In this
172 case, loss of CTCF binding is not caused by CBS mutations or methylation and is
173 accompanied with the decrease of chromatin accessibility. This exemplifies that some
174 additional factors may influence CTCF binding. One potential candidate in Jpx non-coding
175 RNA that regulates CTCF binding to a subset of developmentally sensitive loci by
176 competitive inhibition (Oh et al., 2021a).

177

178 Expansion of repeats and viral DNA integration could also affect the profile of spatial
179 interactions between remote genomic elements. Short tandem repeats (STRs) alter TAD
180 boundaries by modulating CTCF binding (Ibrahim and Mundlos, 2020). In several
181 pathological models, STRs accumulate at TAD boundaries increasing the density of CpG
182 islands which are often hypermethylated in pathologies. One example is the *FMR1* gene,
183 whose repression leads to the fragile X chromosome syndrome (Martin-Bell syndrome). STR
184 accumulation at the boundary of encompassing TAD promotes DNA hypermethylation
185 followed by the decrease of CTCF binding and significant alteration in the enhancer
186 landscape of the locus. These lead to the loss of the TAD boundary and *FMR1* repression
187 (Sun et al., 2018).

188

189 Integration of primate-specific endogenous retrotransposon human endogenous retrovirus
190 subfamily H (HERV-H) was shown to create TAD boundaries in the genome of human
191 pluripotent stem cells (Zhang et al., 2019). In this case, active viral transcription, but not CBS
192 within the viral genome, creates a TAD boundary at the site of the HERV-H integration. This
193 is in line with recent observations showing that active transcription constitutes a barrier for
194 the cohesin-driven extrusion (Brandão et al., 2019). In contrast to HERV-H, insertion of the
195 human T-lymphotropic virus HTLV-1 establishes *de novo* loops due to the presence of CBS
196 within the viral genome. This results in abnormal host gene transcription not only in loci
197 proximal to the integration site, but also more than 300 kb away (Melamed et al., 2018). The
198 same was observed for the bovine leukaemia virus (BLV) carrying several CBSs which were
199 involved in formation of new chromatin loops with the host chromosome loci after the
200 provirus integration (Bellefroid et al., 2022).

201

202 In some cases, violations of CTCF-dependent loop structures could be driven by external
203 factors, such as drug use. For example, cocaine addiction results in a pathogenic looping

204 within the *IRXA* locus in brain neurons due to DNA hypomethylation at a set of CBSs
205 (Vaillancourt et al., 2021).

206

207 Development of some diseases (in particular, cancer) is driven by changes in enhancer-
208 promoter loops established by specific TFs. In melanoma, treatment with a BRAF inhibitor
209 PLX4032 leads to survival and further expansion of cancer cells due to upregulation of the
210 *MET* gene. *MET* is normally expressed in many tissues and cell lines, but treatment of
211 melanoma cells with PLX4032 results in a seven-fold increase of *MET* expression that relies
212 on the activity of a tissue-specific TF MITF. This factor is essential for the spatial contacts
213 between the *MET* promoter and the enhancer located 63 kb away. This interaction triggers
214 the *MET* upregulation and the HGF-MET signalling cascade. MITF depletion, as well as the
215 destruction of its binding site in the *MET* enhancer, restores the sensitivity of melanoma cells
216 to treatment with BRAF inhibitors (Webster et al., 2014). Changes in the expression of
217 *VEGFA*, *MGA1*, *ZFAND3*, *TCF7L2*, *OPEN*, *GLIS3* and others genes due to disruption of
218 their contacts with the enhancer/enhancer hub may contribute to the development of type 2
219 diabetes (Miguel-Escalada et al., 2019).

220 In T-ALL, extended deletions eliminating CTCF-bound topological borders result in aberrant
221 activation of proto-oncogenes *TAL1* and *LMO2* by distal enhancers from adjacent genome
222 loci (Hnisz et al., 2016).

223

224 Disruption of the TAD borders also occurs in Autosomal-dominant adult-onset demyelinating
225 leukodystrophy (ADLD), a disorder characterised by a progressive demyelination of the
226 central nervous system due to cerebral lamin B1 (*LMNB1*) overexpression. A 600-kb
227 deletion eliminating a TAD boundary results in interactions between the three strong
228 enhancers and the *LMNB1* promoter, causing *LMNB1* overexpression and myelin
229 degeneration. In human 6p22.3 locus, deletion of an entire TAD including boundaries,
230 correlated with activation of the *ID4* gene by enhancers from the neighbouring TAD in the

231 developing limb bud resulted in development of mesomelic dysplasia with hypoplastic tibia
232 and fibula (Flöttmann et al., 2015).

233 SVs associated with changes in spatial genomic interactions also cause the Liebenberg
234 syndrome, a limb malformation due to dysregulation of the *PITX1* expression: the forelimbs
235 develop into the hindlimbs. *PITX1* controls the normal development of the hindlimbs where
236 its expression is governed by the interaction with the *Pen* enhancer. In the forelimb buds,
237 *PITX1* is not expressed due to spatial isolation from the *Pen* by the insulator located in the
238 promoter region of the nearby *H2afy* gene. In Liebenberg syndrome, multiple deletions
239 eliminate this insulator allowing the *Pen* enhancer to activate *PITX1* leading to abnormal
240 formation of the forelimb bones and the kneecap near the elbow (Kragesteen et al., 2018,
241 2019).

242

243 Duplications can also affect the TAD profile and/or intra-TAD spatial interactions. In the
244 *SOX9/KCNJ2/KCNJ16* locus, where genes encoding the developmental regulator *SOX9* and
245 potassium channels *KCNJ2/KCNJ16* are located in adjacent TADs, duplications within the
246 *SOX9* TAD result in female to male sex reversal. These duplications encompassing the TAD
247 boundary and the entire *KCNJ2* gene result in the formation of a new TAD, where *KCNJ2* is
248 upregulated by *SOX2*- specific enhancers. This leads to the limb malformations with aplasia
249 of nails and short digits known as Cooks syndrome (Franke et al., 2016). In addition to
250 duplications, a translocation involving the *SOX9/KCNJ2/KCNJ16* locus leads to the Snijders
251 Blok-Campeau syndrome characterized by intellectual disability, speech problems, and
252 distinctive facial features (Melo et al., 2020).

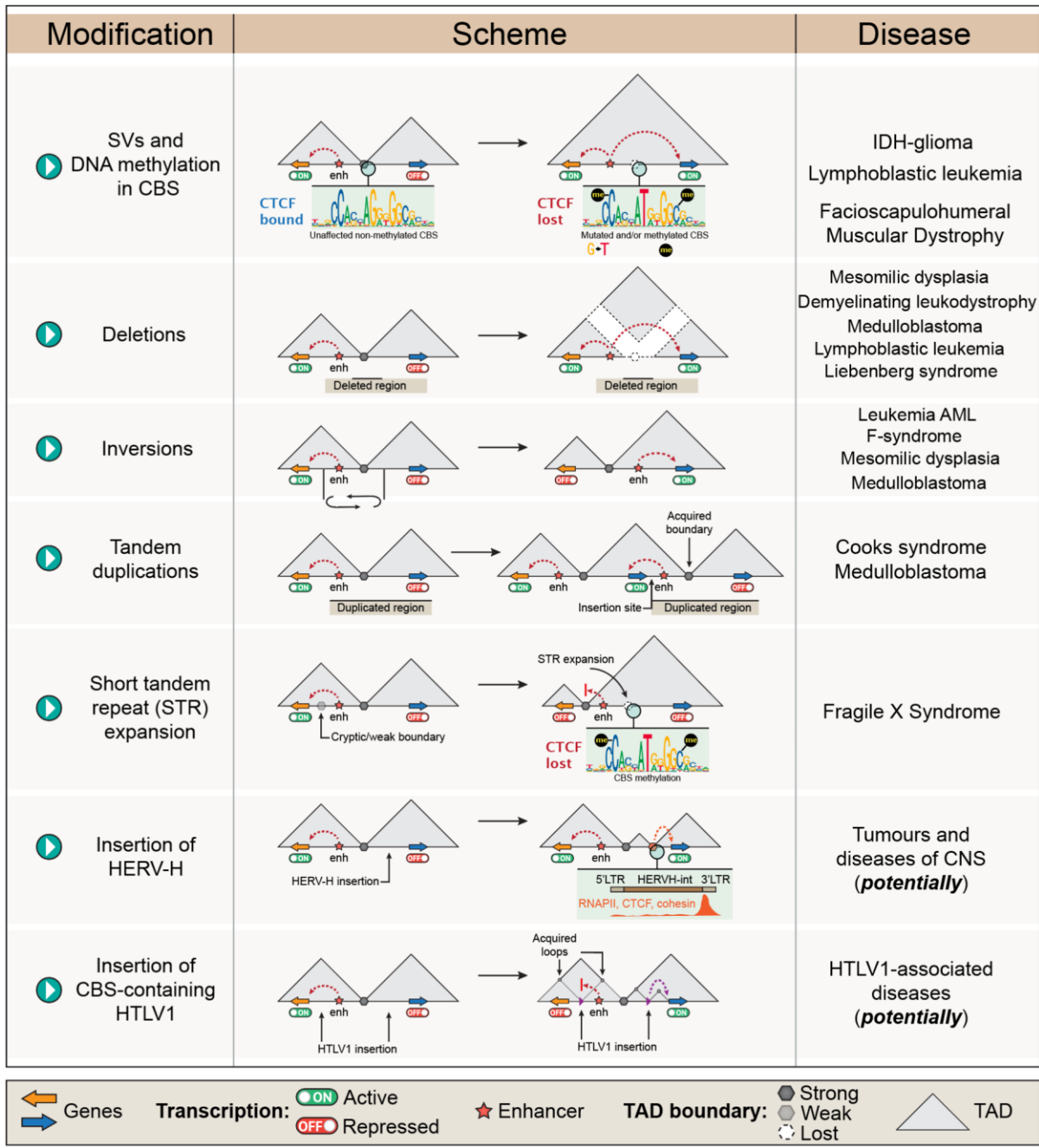
253

254 Numerous SVs lead to the emergence of new TADs within the *YPEL2/LINC01476* locus
255 leading to dysregulation of gene expression manifested in autosomal-dominant retinitis
256 pigmentosa (adRP) (de Bruijn et al., 2020). In some loci, large-scale SVs cause a variety of
257 distinct pathologies. The canonical example is the *WNT6/IHH/EPHA4/PAX3* locus where
258 different deletions, inversions and duplications result in limb malformation. Some of the

259 intergenic SVs induce the F syndrome (acropectorovertebral dysgenesis), a rare inherited
260 skeletal disorder characterized by the fusion of the thumb and index finger. In particular, the
261 disease is caused by an inversion in the *EPHA4* gene locus, which leaves the TAD boundary
262 intact, but places an enhancer from the neighbouring TAD near the *WNT6* gene promoting
263 its overexpression. Other duplications and deletions affecting TAD structure within the
264 regions cause brachydactyly and polydactyly (Lupiáñez et al., 2015).

265 Large-scale inversions lead to the branchiooculofacial syndrome (BOFS), characterised by
266 skin, face and eye defects of varying severity. This pathology occurs when the normal
267 expression of the neural crest regulator *TFAP2A* is impaired. Usually, it is a result of a partial
268 gene deletion, however, a recent study (Laugsch et al., 2019), describes a patient with a 89-
269 Mb inversion that does not affect *TFAP2A per se*, but compromises its expression. This
270 inversion disrupts the original *TFAP2A*-containing TADs and the interaction between the
271 *TFAP2A* gene and a group of its enhancers.

272



273

274 **Figure 2.** TAD-centric view on the 3D genome organization and disease

275 Finally, at a whole-nucleus scale, contacts between non-homologous chromosomes can also

276 lead to oncogenic chromosomal translocations. This disrupts local regulatory 3D interaction

277 networks and alters cellular transcription programs. Few examples include interactions of

278 chromosomes 8 and 14 or chromosomes 11 and 14 in B-lymphocytes leading to Burkitt or

279 mantle cell lymphoma, respectively; chromosomes 12 and 16 in adipocytes leading to

280 t(12;16) in liposarcoma; chromosomes 5 and 6 in hepatocytes leading to t(5;6) in

281 hepatocarcinoma (Allinne et al., 2014; Germini et al., 2017; Kuroda et al., 2004; Parada et
282 al., 2004; Roix et al., 2003).

283

284 Changes in 3D genome organization due to DNA methylation or SV mutations affecting 3D
285 genome can lead to a phenomenon called “enhancer hijacking” when enhancers change
286 their target, leading to gene expression abnormalities and pathologies. For example, a SV in
287 the vicinity of the *GFI1B* gene leads to *GFI1B* interaction with distal superenhancers and
288 overexpression in medulloblastoma (Northcott et al., 2014). Another example of enhancer
289 hijacking associated with rearrangements involving loci encoding the *EVI1* stem-cell
290 regulator and *GATA2*. In particular, inversion/translocation *inv(3)(q21;q26.2)* and
291 *t(3;3)(q21;q26.2)* place the *GATA2* enhancer in a close proximity to the *EVI1* promoter .
292 resulting in *EVI1* overexpression and *GATA2* functional haploinsufficiency in acute myeloid
293 leukemia (AML) cells (Gröschel et al., 2014).

294

295 Together, alterations in the genome 3D organization are quite common in cancer and
296 developmental disorders. Screening revealed that 7.3% of balanced chromosomal
297 abnormalities disrupt TADs at known syndromic loci (Redin et al., 2017), and 14% SVs
298 affecting TAD boundaries in cancers lead to remarkable changes in expression of nearby
299 genes (Akdemir et al., 2020). The ability of naturally occurring SVs to target 3D genome and
300 cause socially-significant diseases imposes the development and further clinical validation of
301 3D genome editing technologies applicable for treating patients.

302

303 **3D genome editing**

304

305 Since alterations in the chromatin contact profiles are associated with many pathologies,
306 development of the 3D genome editing methods is on the frontlines of biomedicine. The

307 existing approaches largely rely on the use of either native architectural proteins such as
308 CTCF or artificial looping proteins.

309

310 As highlighted above, CTCF is a master regulator of the mammalian interphase genome
311 folding (van Ruiten and Rowland, 2021), and thus is a predominant target for the 3D genome
312 engineering. CBS deletion/insertion/inversion and point mutations is a streamlined path for
313 the precise control of the CTCF binding within genome regulatory elements and TAD
314 boundaries/loop anchors (Narendra et al., 2016; Willemin et al., 2021). In several loci, such
315 manipulations alter loop profile and result in changes of gene expression that could be
316 potentially used as a strategy for the cell type-specific transcription reprogramming in
317 patients (Gong et al., 2019). However, genomic DNA editing possesses risks of
318 chromosome rearrangements that should be considered upon the design of clinically-
319 relevant applications (Samuelson et al., 2021).

320

321 In case of *de novo* TAD formation or excessive CTCF binding, depletion of CTCF from
322 particular sites in chromatin can be accomplished through epigenetic modifications of CBS to
323 inhibit CTCF binding without changes in the primary DNA sequence. In this case, chimeric
324 proteins consisting of catalytically dead Cas9 (dCas9) fused with the Krüppel-associated box
325 (KRAB), a H3K9me3-catalyzing repressor (dCas9-KRAB) or DNA-methyltransferases
326 DNMT3A and DNMT3AL were shown to be effective inhibitors of CTCF binding when
327 precisely targeted to the CBS (Liu et al., 2016; Tarjan et al., 2019).

328

329 Another possibility that is developed for potential clinical applications is the usage of small
330 molecules interfering with the CTCF binding. Cell treatment with the anti-cancer agent
331 curaxin CBL0137 leads to a partial depletion of CTCF from chromatin and compromises
332 enhancer-promoter contacts (Kantidze et al., 2019). This opens an avenue for the rational *in*
333 *silico* design of drugs acting as inhibitors of DNA binding and competitors for the protein-
334 protein interactions for the major players in the 3D genome maintenance.

335

336 Since some diseases are associated with the decrease of CTCF occupancy at particular
337 CBSs (Miyata et al., 2021), stabilisation of CTCF binding at such loci is a strategy to be
338 considered. Several post-translational modifications are essential for the CTCF insulator and
339 barrier activities (Pavlaki et al., 2018). Indeed, mutations in the CTCF region subjected to
340 poly(ADP-ribosyl)ation by PARP1 compromise cohesin enrichment at CBSs, i.e. interfere
341 with cohesin/CTCF-dependent loop formation (Pugacheva et al., 2020). In the Epstein Barr
342 virus genome, PARP1 acts to stabilize CTCF binding at particular sites (Lupey-Green et al.,
343 2018). Thus, inducible recruitment of PARP1 to certain CBSs could be a tool for the
344 stabilization of selective CTCF binding to these sites. Other post-translational modifications
345 of CTCF such as SUMOylation and phosphorylation (Kitchen and Schoenherr, 2010; Luo et
346 al., 2020) are also of interest for the 3D genome manipulation in both genome-wide and
347 locus-specific manner. Together, these examples illustrate that epigenome targeting and
348 inducible CTCF post-translational modifications could potentially serve as a proxy for the 3D
349 genome editing.

350

351 A number of diseases are characterized by a complete loss of CBSs at critical regulatory
352 elements due to deletions and other SVs (Dahlqvist et al., 2021; Guo et al., 2018; Ushiki et
353 al., 2021). In such cases, recruitment of CTCF by an unrelated DNA-binding module and
354 restoration of the original loop profile might be a potential treatment strategy. One example is
355 a dCas9-mediated CTCF recruitment enforced by the coupling with the SunTag technology
356 allowing recruitment of multiple CTCF molecules to the same binding site (Oh et al., 2021b).
357 This method has been tested in the *TFF* locus associated with breast, lung and colon
358 cancers (Xu et al., 2013) and demonstrated a potential utility for the 3D genome engineering
359 in multigene disease-associated loci.

360

361 Some pathologies are accompanied by a total loss of *CTCF* expression followed by genome-
362 wide alterations of chromatin 3D structure. Consequently, insertion of a functional CTCF

363 gene could restore an original loop pattern of the affected loci. For example, breast cancer
364 could be inhibited by the increased *CTCF* expression; the *CTCF* gene is frequently deleted
365 in this type of cancer and this negatively affects the survival rate of patients at late stages
366 (Duan et al., 2022). *CTCF* gene insertion by pseudoviruses also slows down the cancer cell
367 divisions and/or migration, as well as metastasis in the lungs and brain, and affects the
368 expression of almost 130 genes.

369

370 An alternative approach for manipulation of the 3D genome architecture relies on the
371 expression of chimeric proteins containing DNA-binding modules (ZF, TALE, dCas9) fused
372 with units forming homo- or heterodimers, such as dimerization domains of mammalian
373 transcription factors, e.g. the self-associating (SA) domain of the Ldb1 protein (Deng et al.,
374 2014). These chimeric proteins form relatively stable dimers and are suitable for the
375 formation of constant distant interactions in chromatin. These contacts can be made
376 reversible *via* inducible polymerization. One example is CLOuD9 chromatin loop
377 reorganisation system where PYL1 and ABI1 fused with two different dCas modules interact
378 with each other in the presence of abscisic acid (ABA). Application of the CLOuD9 system to
379 the *Oct4* locus associated with various types of cancers demonstrated that recruitment of
380 these fusion proteins to the *Oct4* promoter and its distal enhancer induced loop formation
381 and upregulation of *Oct4* after ABA addition (Morgan et al., 2017). A similar approach, LADL
382 (light-activated dynamic looping), utilizes co-expression of cryptochrome 2 (CRY2) and
383 truncated CIB1 (CIBN) fused to dCas9. Exposure of cells to 470-nm blue light induces
384 dimerization of CRY2, and heteromerization of CRY2 and CIBN. As a result, loci targeted by
385 dCas9-CIBN form a transient loop. In a proof-of-concept study, LADL-induced looping
386 between *Zfp462* and the *Klf4* superenhancer in mouse embryonic stem cells was
387 successfully used to increase the *Zfp462* expression (Kim et al., 2019).

388

389 **Concluding remarks**

390

391 Genome-wide association studies revealed a number of genomic SVs associated with the
392 development of various diseases. Most of these SVs are located outside genes and their
393 regulatory modules. Consequently, the mechanical links between disease-associated SV
394 and regulation of genome activity remained obscure. Recent results discussed here argue
395 that many of the disease-associated SVs affect the 3D genome organization. This raises the
396 issue of the need for 3D genome editing. Several approaches for such editing have been
397 proposed and tested on cell cultures. The question is whether any of the developed
398 strategies has the prospect of practical application in the treatment of patients. In the case of
399 cancer, the straightforward strategy is to kill a cancer cell if it can be recognized and targeted
400 rather than to try to correct anything in this cell. The only possible application here is to use
401 low molecular weight agents (ex: curaxins) that affect all cells with some preference to
402 cancer cells. More interesting opportunities for practical applications of 3D genome editing
403 arise in cases where it is necessary to deliver to the organism its own normal cells, which will
404 exist alongside corrupted ones or replace them. This strategy assumes that damaged cells
405 are taken from the patient, manipulated in the laboratory and returned to the patient's body.
406 In the future, this approach could be useful for the treatment of a number of diseases of the
407 hematopoietic and endocrine organs, as well as some types of muscular dystrophies.

408

409 **Acknowledgements**

410 GRANTS: This work was supported by the Russian Science Foundation (21-64-00001) and
411 by the Russian Ministry of Science and Higher Education (075-15-2021-1062) to SU and
412 from the AFM (CTCFSHD) and the IDB RAS Government basic research programs (0088-
413 2022- 0007 and 0088- 2022- 0016) to YV.

414

415 **References**

416 Akdemir, K.C., Le, V.T., Chandran, S., Li, Y., Verhaak, R.G., Beroukhir, R., Campbell, P.J.,
417 Chin, L., Dixon, J.R., Futreal, P.A., et al. (2020). Disruption of chromatin folding domains by
418 somatic genomic rearrangements in human cancer. *Nat. Genet.* 52, 294–305.

419 <https://doi.org/10.1038/s41588-019-0564-y>.

420 Albiez, H., Cremer, M., Tiberi, C., Vecchio, L., Schermelleh, L., Dittrich, S., Küpper, K., Joffe,
421 B., Thormeyer, T., von Hase, J., et al. (2006). Chromatin domains and the interchromatin
422 compartment form structurally defined and functionally interacting nuclear networks.
423 *Chromosome Res.* 14, 707–733. <https://doi.org/10.1007/s10577-006-1086-x>.

424 Allinne, J., Pichugin, A., Iarovaia, O., Klibi, M., Barat, A., Zlotek-Zlotkiewicz, E.,
425 Markozashvili, D., Petrova, N., Camara-Clayette, V., Loudinkova, E., et al. (2014).
426 Perinucleolar relocalization and nucleolin as crucial events in the transcriptional activation of
427 key genes in mantle cell lymphoma. *Blood* 123, 2044–2053. [https://doi.org/10.1182/blood-](https://doi.org/10.1182/blood-2013-06-510511)
428 [2013-06-510511](https://doi.org/10.1182/blood-2013-06-510511).

429 Amândio, A.R., Lopez-Delisle, L., Bolt, C.C., Mascrez, B., and Duboule, D. (2020). A
430 complex regulatory landscape involved in the development of mammalian external genitals.
431 *ELife* 9, e52962. <https://doi.org/10.7554/eLife.52962>.

432 Bauer, B.W., Davidson, I.F., Canena, D., Wutz, G., Tang, W., Litos, G., Horn, S.,
433 Hinterdorfer, P., and Peters, J.-M. (2021). Cohesin mediates DNA loop extrusion by a “swing
434 and clamp” mechanism. *Cell* 184, 5448-5464.e22. <https://doi.org/10.1016/j.cell.2021.09.016>.

435 Bellefroid, M., Rodari, A., Galais, M., Krijger, P.H.L., Tjalsma, S.J.D., Nestola, L., Plant, E.,
436 Vos, E.S.M., Cristinelli, S., Van Driessche, B., et al. (2022). Role of the cellular factor CTCF
437 in the regulation of bovine leukemia virus latency and three-dimensional chromatin
438 organization. *Nucleic Acids Res.* 50, 3190–3202. <https://doi.org/10.1093/nar/gkac107>.

439 Bintu, B., Mateo, L.J., Su, J.-H., Sinnott-Armstrong, N.A., Parker, M., Kinrot, S., Yamaya, K.,
440 Boettiger, A.N., and Zhuang, X. (2018). Super-resolution chromatin tracing reveals domains
441 and cooperative interactions in single cells. *Science* 362, eaau1783.
442 <https://doi.org/10.1126/science.aau1783>.

443 Bonev, B., Mendelson Cohen, N., Szabo, Q., Fritsch, L., Papadopoulos, G.L., Lubling, Y.,
444 Xu, X., Lv, X., Hugnot, J.-P., Tanay, A., et al. (2017). Multiscale 3D Genome Rewiring during
445 Mouse Neural Development. *Cell* 171, 557-572.e24.
446 <https://doi.org/10.1016/j.cell.2017.09.043>.

447 Boyle, S., Gilchrist, S., Bridger, J.M., Mahy, N.L., Ellis, J.A., and Bickmore, W.A. (2001). The
448 spatial organization of human chromosomes within the nuclei of normal and emerin-mutant
449 cells. *Hum Mol Genet* 10, 211–219. .

450 Brandão, H.B., Paul, P., van den Berg, A.A., Rudner, D.Z., Wang, X., and Mirny, L.A. (2019).
451 RNA polymerases as moving barriers to condensin loop extrusion. *Proc. Natl. Acad. Sci. U.*
452 *S. A.* 116, 20489–20499. <https://doi.org/10.1073/pnas.1907009116>.

453 de Bruijn, S.E., Fiorentino, A., Ottaviani, D., Fanucchi, S., Melo, U.S., Corral-Serrano, J.C.,
454 Mulders, T., Georgiou, M., Rivolta, C., Pontikos, N., et al. (2020). Structural Variants Create
455 New Topological-Associated Domains and Ectopic Retinal Enhancer-Gene Contact in
456 Dominant Retinitis Pigmentosa. *Am. J. Hum. Genet.* 107, 802–814.
457 <https://doi.org/10.1016/j.ajhg.2020.09.002>.

458 Crosetto, N., and Bienko, M. (2020). Radial Organization in the Mammalian Nucleus. *Front.*
459 *Genet.* 11, 33. <https://doi.org/10.3389/fgene.2020.00033>.

460 Dahlqvist, J., Fulco, C.P., Ray, J.P., Liechti, T., de Boer, C.G., Lieb, D.J., Eisenhaure, T.M.,
461 Engreitz, J.M., Roederer, M., and Hacohen, N. (2021). Systematic identification of genomic
462 elements that regulate FCGR2A expression and harbor variants linked with autoimmune
463 disease. *Hum. Mol. Genet.* ddab372. <https://doi.org/10.1093/hmg/ddab372>.

464 Davidson, I.F., Bauer, B., Goetz, D., Tang, W., Wutz, G., and Peters, J.-M. (2019). DNA loop
465 extrusion by human cohesin. *Science* 366, 1338–1345.
466 <https://doi.org/10.1126/science.aaz3418>.

467 Deng, W., Rupon, J.W., Krivega, I., Breda, L., Motta, I., Jahn, K.S., Reik, A., Gregory, P.D.,
468 Rivella, S., Dean, A., et al. (2014). Reactivation of Developmentally Silenced Globin Genes
469 by Forced Chromatin Looping. *Cell* 158, 849–860. <https://doi.org/10.1016/j.cell.2014.05.050>.

470 Dillinger, S., Straub, T., and Németh, A. (2017). Nucleolus association of chromosomal
471 domains is largely maintained in cellular senescence despite massive nuclear
472 reorganisation. *PLoS ONE* 12, e0178821. <https://doi.org/10.1371/journal.pone.0178821>.

473 Dixon, J.R., Jung, I., Selvaraj, S., Shen, Y., Antosiewicz-Bourget, J.E., Lee, A.Y., Ye, Z.,
474 Kim, A., Rajagopal, N., Xie, W., et al. (2015). Chromatin architecture reorganization during

475 stem cell differentiation. *Nature* 518, 331–336. <https://doi.org/10.1038/nature14222>.

476 Dixon, J.R., Gorkin, D.U., and Ren, B. (2016). Chromatin Domains: The Unit of
477 Chromosome Organization. *Mol. Cell* 62, 668–680.
478 <https://doi.org/10.1016/j.molcel.2016.05.018>.

479 Duan, J., Bao, C., Xie, Y., Guo, H., Liu, Y., Li, J., Liu, R., Li, P., Bai, J., Yan, Y., et al. (2022).
480 Targeted core-shell nanoparticles for precise CTCF gene insert in treatment of metastatic
481 breast cancer. *Bioact. Mater.* 11, 1–14. <https://doi.org/10.1016/j.bioactmat.2021.10.007>.

482 Flavahan, W.A., Drier, Y., Liao, B.B., Gillespie, S.M., Venteicher, A.S., Stemmer-
483 Rachamimov, A.O., Suvà, M.L., and Bernstein, B.E. (2016). Insulator dysfunction and
484 oncogene activation in IDH mutant gliomas. *Nature* 529, 110–114.
485 <https://doi.org/10.1038/nature16490>.

486 Flöttmann, R., Wagner, J., Kobus, K., Curry, C.J., Savarirayan, R., Nishimura, G., Yasui, N.,
487 Spranger, J., Van Esch, H., Lyons, M.J., et al. (2015). Microdeletions on 6p22.3 are
488 associated with mesomelic dysplasia Savarirayan type. *J. Med. Genet.* 52, 476–483.
489 <https://doi.org/10.1136/jmedgenet-2015-103108>.

490 Franke, M., Ibrahim, D.M., Andrey, G., Schwarzer, W., Heinrich, V., Schöpflin, R., Kraft, K.,
491 Kempfer, R., Jerković, I., Chan, W.-L., et al. (2016). Formation of new chromatin domains
492 determines pathogenicity of genomic duplications. *Nature* 538, 265–269.
493 <https://doi.org/10.1038/nature19800>.

494 Gacita, A.M., Fullenkamp, D.E., Ohiri, J., Pottinger, T., Puckelwartz, M.J., Nobrega, M.A.,
495 and McNally, E.M. (2021). Genetic Variation in Enhancers Modifies Cardiomyopathy Gene
496 Expression and Progression. *Circulation* 143, 1302–1316.
497 <https://doi.org/10.1161/CIRCULATIONAHA.120.050432>.

498 Germini, D., Tsfasman, T., Klibi, M., El-Amine, R., Pichugin, A., Iarovaia, O.V.V., Bilhou-
499 Nabera, C., Subra, F., Bou Saada, Y., Sukhanova, A., et al. (2017). HIV Tat induces a
500 prolonged MYC relocalization next to IGH in circulating B-cells. *Leukemia* 31, 2515–2522.
501 <https://doi.org/10.1038/leu.2017.106>.

502 Gómez-Marín, C., Tena, J.J., Acemel, R.D., López-Mayorga, M., Naranjo, S., de la Calle-

503 Mustienes, E., Maeso, I., Beccari, L., Aneas, I., Vielmas, E., et al. (2015). Evolutionary
504 comparison reveals that diverging CTCF sites are signatures of ancestral topological
505 associating domains borders. *Proc. Natl. Acad. Sci. U. S. A.* *112*, 7542–7547.
506 <https://doi.org/10.1073/pnas.1505463112>.

507 Gong, W., Liu, Y., Qu, H., Liu, A., Sun, P., and Wang, X. (2019). The effect of CTCF binding
508 sites destruction by CRISPR/Cas9 on transcription of metallothionein gene family in liver
509 hepatocellular carcinoma. *Biochem. Biophys. Res. Commun.* *510*, 530–538.
510 <https://doi.org/10.1016/j.bbrc.2019.01.107>.

511 Gröschel, S., Sanders, M.A., Hoogenboezem, R., de Wit, E., Bouwman, B.A.M., Erpelinck,
512 C., van der Velden, V.H.J., Havermans, M., Avellino, R., van Lom, K., et al. (2014). A Single
513 Oncogenic Enhancer Rearrangement Causes Concomitant EVI1 and GATA2 Deregulation
514 in Leukemia. *Cell* *157*, 369–381. <https://doi.org/10.1016/j.cell.2014.02.019>.

515 Guelen, L., Pagie, L., Brasset, E., Meuleman, W., Faza, M.B., Talhout, W., Eussen, B.H., de
516 Klein, A., Wessels, L., de Laat, W., et al. (2008). Domain organization of human
517 chromosomes revealed by mapping of nuclear lamina interactions. *Nature* *453*, 948–951.
518 <https://doi.org/10.1038/nature06947>.

519 Guo, Y.A., Chang, M.M., Huang, W., Ooi, W.F., Xing, M., Tan, P., and Skanderup, A.J.
520 (2018). Mutation hotspots at CTCF binding sites coupled to chromosomal instability in
521 gastrointestinal cancers. *Nat. Commun.* *9*, 1520. [https://doi.org/10.1038/s41467-018-03828-](https://doi.org/10.1038/s41467-018-03828-2)
522 [2](https://doi.org/10.1038/s41467-018-03828-2).

523 Himeda, C.L., Jones, T.I., and Jones, P.L. (2014). Fascioscapulohumeral muscular
524 dystrophy as a model for epigenetic regulation and disease. *Antioxid. Redox Signal.*
525 <https://doi.org/10.1089/ars.2014.6090>.

526 Hnisz, D., Weintraub, A.S., Day, D.S., Valton, A.-L., Bak, R.O., Li, C.H., Goldmann, J.,
527 Lajoie, B.R., Fan, Z.P., Sigova, A.A., et al. (2016). Activation of proto-oncogenes by
528 disruption of chromosome neighborhoods. *Science* *351*, 1454–1458.
529 <https://doi.org/10.1126/science.aad9024>.

530 Hnisz, D., Shrinivas, K., Young, R.A., Chakraborty, A.K., and Sharp, P.A. (2017). A phase

531 separation model predicts key features of transcriptional control. *Cell* 169, 13–23.
532 <https://doi.org/10.1016/j.cell.2017.02.007>.

533 Hsieh, T.-H.S., Cattoglio, C., Slobodyanyuk, E., Hansen, A.S., Rando, O.J., Tjian, R., and
534 Darzacq, X. (2020). Resolving the 3D Landscape of Transcription-Linked Mammalian
535 Chromatin Folding. *Mol. Cell* 78, 539-553.e8. <https://doi.org/10.1016/j.molcel.2020.03.002>.

536 Ibrahim, D.M., and Mundlos, S. (2020). Three-dimensional chromatin in disease: What holds
537 us together and what drives us apart? *Curr. Opin. Cell Biol.* 64, 1–9.
538 <https://doi.org/10.1016/j.ceb.2020.01.003>.

539 Kantidze, O.L., Luzhin, A.V., Nizovtseva, E.V., Safina, A., Valieva, M.E., Golov, A.K.,
540 Velichko, A.K., Lyubitelev, A.V., Feofanov, A.V., Gurova, K.V., et al. (2019). The anti-cancer
541 drugs curaxins target spatial genome organization. *Nat. Commun.* 10, 1441.
542 <https://doi.org/10.1038/s41467-019-09500-7>.

543 Kim, H.-J., Yardımcı, G.G., Bonora, G., Ramani, V., Liu, J., Qiu, R., Lee, C., Hesson, J.,
544 Ware, C.B., Shendure, J., et al. (2020). Capturing cell type-specific chromatin compartment
545 patterns by applying topic modeling to single-cell Hi-C data. *PLoS Comput. Biol.* 16,
546 e1008173. <https://doi.org/10.1371/journal.pcbi.1008173>.

547 Kim, J.H., Rege, M., Valeri, J., Dunagin, M.C., Metzger, A., Titus, K.R., Gilgenast, T.G.,
548 Gong, W., Beagan, J.A., Raj, A., et al. (2019). LADL: light-activated dynamic looping for
549 endogenous gene expression control. *Nat. Methods* 16, 633–639.
550 <https://doi.org/10.1038/s41592-019-0436-5>.

551 Kisseljova, N.P., Dmitriev, P., Katargin, A., Kim, E., Ezerina, D., Markozashvili, D.,
552 Malysheva, D., Planche, E., Lemmers, R.J.L.F., van der Maarel, S.M., et al. (2014). DNA
553 polymorphism and epigenetic marks modulate the affinity of a scaffold/matrix attachment
554 region to the nuclear matrix. *Eur J Hum Genet* 22, 1117–1123.
555 <https://doi.org/10.1038/ejhg.2013.306>.

556 Kitchen, N.S., and Schoenherr, C.J. (2010). Sumoylation modulates a domain in CTCF that
557 activates transcription and decondenses chromatin. *J. Cell. Biochem.* 111, 665–675.
558 <https://doi.org/10.1002/jcb.22751>.

559 Kloetgen, A., Thandapani, P., Ntziachristos, P., Ghebrechristos, Y., Nomikou, S., Lazaris, C.,
560 Chen, X., Hu, H., Bakogianni, S., Wang, J., et al. (2020). Three-dimensional chromatin
561 landscapes in T cell acute lymphoblastic leukemia. *Nat. Genet.* *52*, 388–400.
562 <https://doi.org/10.1038/s41588-020-0602-9>.

563 Kragestein, B.K., Spielmann, M., Paliou, C., Heinrich, V., Schöpflin, R., Esposito, A.,
564 Annunziatella, C., Bianco, S., Chiariello, A.M., Jerković, I., et al. (2018). Dynamic 3D
565 chromatin architecture contributes to enhancer specificity and limb morphogenesis. *Nat.*
566 *Genet.* *50*, 1463–1473. <https://doi.org/10.1038/s41588-018-0221-x>.

567 Kragestein, B.K., Brancati, F., Digilio, M.C., Mundlos, S., and Spielmann, M. (2019). H2AFY
568 promoter deletion causes PITX1 endoactivation and Liebenberg syndrome. *J. Med. Genet.*
569 *56*, 246–251. <https://doi.org/10.1136/jmedgenet-2018-105793>.

570 Krietenstein, N., Abraham, S., Venev, S.V., Abdennur, N., Gibcus, J., Hsieh, T.-H.S., Parsi,
571 K.M., Yang, L., Maehr, R., Mirny, L.A., et al. (2020). Ultrastructural Details of Mammalian
572 Chromosome Architecture. *Mol. Cell* *78*, 554-565.e7.
573 <https://doi.org/10.1016/j.molcel.2020.03.003>.

574 Kuroda, M., Tanabe, H., Yoshida, K., Oikawa, K., Saito, A., Kiyuna, T., Mizusawa, H., and
575 Mukai, K. (2004). Alteration of chromosome positioning during adipocyte differentiation. *J.*
576 *Cell Sci.* *117*, 5897–5903. <https://doi.org/10.1242/jcs.01508>.

577 Laugsch, M., Bartusel, M., Rehimi, R., Alirzayeva, H., Karaolidou, A., Crispatzu, G., Zentis,
578 P., Nikolic, M., Bleckwehl, T., Kolovos, P., et al. (2019). Modeling the Pathological Long-
579 Range Regulatory Effects of Human Structural Variation with Patient-Specific hiPSCs. *Cell*
580 *Stem Cell* *24*, 736-752.e12. <https://doi.org/10.1016/j.stem.2019.03.004>.

581 Li, Y., Ma, C., Li, S., Wang, J., Li, W., Yang, Y., Li, X., Liu, J., Yang, J., Liu, Y., et al. (2022).
582 Regulatory Variant rs2535629 in ITIH3 Intron Confers Schizophrenia Risk By Regulating
583 CTCF Binding and SFMBT1 Expression. *Adv. Sci. Weinh. Baden-Wurt. Ger.* e2104786.
584 <https://doi.org/10.1002/advs.202104786>.

585 Lieberman-Aiden, E., van Berkum, N.L., Williams, L., Imakaev, M., Ragoczy, T., Telling, A.,
586 Amit, I., Lajoie, B.R., Sabo, P.J., Dorschner, M.O., et al. (2009). Comprehensive mapping of

587 long range interactions reveals folding principles of the human genome. *Science* 326, 289–
588 293. <https://doi.org/10.1126/science.1181369>.

589 Liu, X.S., Wu, H., Ji, X., Stelzer, Y., Wu, X., Czauderna, S., Shu, J., Dadon, D., Young, R.A.,
590 and Jaenisch, R. (2016). Editing DNA Methylation in the Mammalian Genome. *Cell* 167,
591 233-247.e17. <https://doi.org/10.1016/j.cell.2016.08.056>.

592 Luo, H., Yu, Q., Liu, Y., Tang, M., Liang, M., Zhang, D., Xiao, T.S., Wu, L., Tan, M., Ruan,
593 Y., et al. (2020). LATS kinase-mediated CTCF phosphorylation and selective loss of
594 genomic binding. *Sci. Adv.* 6, eaaw4651. <https://doi.org/10.1126/sciadv.aaw4651>.

595 Lupey-Green, L.N., Caruso, L.B., Madzo, J., Martin, K.A., Tan, Y., Hulse, M., and Tempera,
596 I. (2018). PARP1 Stabilizes CTCF Binding and Chromatin Structure To Maintain Epstein-
597 Barr Virus Latency Type. *J. Virol.* 92, e00755-18. <https://doi.org/10.1128/JVI.00755-18>.

598 Lupiáñez, D.G., Kraft, K., Heinrich, V., Krawitz, P., Brancati, F., Klopocki, E., Horn, D.,
599 Kayserili, H., Opitz, J.M., Laxova, R., et al. (2015). Disruptions of topological chromatin
600 domains cause pathogenic rewiring of gene-enhancer interactions. *Cell* 161, 1012–1025.
601 <https://doi.org/10.1016/j.cell.2015.04.004>.

602 Melamed, A., Yaguchi, H., Miura, M., Witkover, A., Fitzgerald, T.W., Birney, E., and
603 Bangham, C.R. (2018). The human leukemia virus HTLV-1 alters the structure and
604 transcription of host chromatin in cis. *ELife* 7, e36245. <https://doi.org/10.7554/eLife.36245>.

605 Melo, U.S., Schöpflin, R., Acuna-Hidalgo, R., Mensah, M.A., Fischer-Zirnsak, B., Holtgrewe,
606 M., Klever, M.-K., Türkmen, S., Heinrich, V., Pluym, I.D., et al. (2020). Hi-C Identifies
607 Complex Genomic Rearrangements and TAD-Shuffling in Developmental Diseases. *Am. J.*
608 *Hum. Genet.* 106, 872–884. <https://doi.org/10.1016/j.ajhg.2020.04.016>.

609 Merkschlager, M., and Nora, E.P. (2016). CTCF and Cohesin in Genome Folding and
610 Transcriptional Gene Regulation. *Annu. Rev. Genomics Hum. Genet.* 17, 17–43.
611 <https://doi.org/10.1146/annurev-genom-083115-022339>.

612 Miguel-Escalada, I., Bonàs-Guarch, S., Cebola, I., Ponsa-Cobas, J., Mendieta-Esteban, J.,
613 Atla, G., Javierre, B.M., Rolando, D.M.Y., Farabella, I., Morgan, C.C., et al. (2019). Human
614 pancreatic islet three-dimensional chromatin architecture provides insights into the genetics

615 of type 2 diabetes. *Nat. Genet.* 51, 1137–1148. <https://doi.org/10.1038/s41588-019-0457-0>.

616 Miyata, K., Imai, Y., Hori, S., Nishio, M., Loo, T.M., Okada, R., Yang, L., Nakadai, T.,
617 Maruyama, R., Fujii, R., et al. (2021). Pericentromeric noncoding RNA changes DNA binding
618 of CTCF and inflammatory gene expression in senescence and cancer. *Proc. Natl. Acad.*
619 *Sci. U. S. A.* 118, e2025647118. <https://doi.org/10.1073/pnas.2025647118>.

620 Morgan, S.L., Mariano, N.C., Bermudez, A., Arruda, N.L., Wu, F., Luo, Y., Shankar, G., Jia,
621 L., Chen, H., Hu, J.-F., et al. (2017). Manipulation of nuclear architecture through CRISPR-
622 mediated chromosomal looping. *Nat. Commun.* 8, 15993.
623 <https://doi.org/10.1038/ncomms15993>.

624 Narendra, V., Bulajić, M., Dekker, J., Mazzoni, E.O., and Reinberg, D. (2016). CTCF-
625 mediated topological boundaries during development foster appropriate gene regulation.
626 *Genes Dev.* 30, 2657–2662. <https://doi.org/10.1101/gad.288324.116>.

627 Nichols, M.H., and Corces, V.G. (2021). Principles of 3D compartmentalization of the human
628 genome. *Cell Rep.* 35, 109330. <https://doi.org/10.1016/j.celrep.2021.109330>.

629 Nieboer, M.M., and de Ridder, J. (2020). svMIL: predicting the pathogenic effect of TAD
630 boundary-disrupting somatic structural variants through multiple instance learning.
631 *Bioinforma. Oxf. Engl.* 36, i692–i699. <https://doi.org/10.1093/bioinformatics/btaa802>.

632 Nora, E.P., Goloborodko, A., Valton, A.-L., Gibcus, J.H., Uebersohn, A., Abdennur, N.,
633 Dekker, J., Mirny, L.A., and Bruneau, B.G. (2017). Targeted degradation of CTCF decouples
634 local insulation of chromosome domains from genomic compartmentalization. *Cell* 169, 930-
635 944.e22. <https://doi.org/10.1016/j.cell.2017.05.004>.

636 Northcott, P.A., Lee, C., Zichner, T., Stütz, A.M., Erkek, S., Kawauchi, D., Shih, D.J.H.,
637 Hovestadt, V., Zapatka, M., Sturm, D., et al. (2014). Enhancer hijacking activates GFI1
638 family oncogenes in medulloblastoma. *Nature* 511, 428–434.
639 <https://doi.org/10.1038/nature13379>.

640 Nuebler, J., Fudenberg, G., Imakaev, M., Abdennur, N., and Mirny, L.A. (2018). Chromatin
641 organization by an interplay of loop extrusion and compartmental segregation. *Proc. Natl.*
642 *Acad. Sci. U. S. A.* 115, E6697–E6706. <https://doi.org/10.1073/pnas.1717730115>.

643 Oh, H.J., Aguilar, R., Kesner, B., Lee, H.-G., Kriz, A.J., Chu, H.-P., and Lee, J.T. (2021a).
644 Jpx RNA regulates CTCF anchor site selection and formation of chromosome loops. *Cell*
645 *184*, 6157-6173.e24. <https://doi.org/10.1016/j.cell.2021.11.012>.

646 Oh, S., Shao, J., Mitra, J., Xiong, F., D'Antonio, M., Wang, R., Garcia-Bassets, I., Ma, Q.,
647 Zhu, X., Lee, J.-H., et al. (2021b). Enhancer release and retargeting activates disease-
648 susceptibility genes. *Nature* *595*, 735–740. <https://doi.org/10.1038/s41586-021-03577-1>.

649 Parada, L.A., McQueen, P.G., and Misteli, T. (2004). Tissue-specific spatial organization of
650 genomes. *Genome Biol.* *5*, R44. <https://doi.org/10.1186/gb-2004-5-7-r44>.

651 Pavlaki, I., Docquier, F., Chernukhin, I., Kita, G., Gretton, S., Clarkson, C.T., Teif, V.B., and
652 Klenova, E. (2018). Poly(ADP-ribosyl)ation associated changes in CTCF-chromatin binding
653 and gene expression in breast cells. *Biochim. Biophys. Acta Gene Regul. Mech.* *1861*, 718–
654 730. <https://doi.org/10.1016/j.bbagrm.2018.06.010>.

655 Petrov, A., Pirozhkova, I., Carnac, G., Laoudj, D., Lipinski, M., and Vassetzky, Y.S. (2006).
656 Chromatin loop domain organization within the 4q35 locus in facioscapulohumeral dystrophy
657 patients versus normal human myoblasts. *Proc. Natl. Acad. Sci. U. S. A.* *103*, 6982–6987.
658 <https://doi.org/10.1073/pnas.0511235103>.

659 Petrov, A., Allinne, J., Pirozhkova, I., Laoudj, D., Lipinski, M., and Vassetzky, Y.S. (2008). A
660 nuclear matrix attachment site in the 4q35 locus has an enhancer-blocking activity in vivo:
661 implications for the facio-scapulo-humeral dystrophy. *Genome Res.* *18*, 39–45.
662 <https://doi.org/10.1101/gr.6620908>.

663 Pugacheva, E.M., Kubo, N., Loukinov, D., Tajmul, M., Kang, S., Kovalchuk, A.L., Strunnikov,
664 A.V., Zentner, G.E., Ren, B., and Lobanenkov, V.V. (2020). CTCF mediates chromatin
665 looping via N-terminal domain-dependent cohesin retention. *Proc. Natl. Acad. Sci. U. S. A.*
666 *117*, 2020–2031. <https://doi.org/10.1073/pnas.1911708117>.

667 Rao, S.S.P., Huntley, M.H., Durand, N.C., Stamenova, E.K., Bochkov, I.D., Robinson, J.T.,
668 Sanborn, A., Machol, I., Omer, A.D., Lander, E.S., et al. (2014). A three-dimensional map of
669 the human genome at kilobase resolution reveals principles of chromatin looping. *Cell* *159*,
670 1665–1680. <https://doi.org/10.1016/j.cell.2014.11.021>.

671 Razin, S.V., and Gavrilov, A.A. (2020). The Role of Liquid-Liquid Phase Separation in the
672 Compartmentalization of Cell Nucleus and Spatial Genome Organization. *Biochem.*
673 *Biokhimiia* 85, 643–650. <https://doi.org/10.1134/S0006297920060012>.

674 Razin, S.V., Gavrilov, A.A., Vassetzky, Y.S., and Ulianov, S.V. (2016). Topologically-
675 associating domains: gene warehouses adapted to serve transcriptional regulation.
676 *Transcription* 7, 84–90. <https://doi.org/10.1080/21541264.2016.1181489>.

677 Redin, C., Brand, H., Collins, R.L., Kammin, T., Mitchell, E., Hodge, J.C., Hanscom, C.,
678 Pillalamarri, V., Seabra, C.M., Abbott, M.-A., et al. (2017). The genomic landscape of
679 balanced cytogenetic abnormalities associated with human congenital anomalies. *Nat.*
680 *Genet.* 49, 36–45. <https://doi.org/10.1038/ng.3720>.

681 Ricci, M.A., Manzo, C., García-Parajo, M.F., Lakadamyali, M., and Cosma, M.P. (2015).
682 Chromatin Fibers Are Formed by Heterogeneous Groups of Nucleosomes In Vivo. *Cell* 160,
683 1145–1158. <https://doi.org/10.1016/j.cell.2015.01.054>.

684 Roix, J.J., McQueen, P.G., Munson, P.J., Parada, L.A., and Misteli, T. (2003). Spatial
685 proximity of translocation-prone gene loci in human lymphomas. *Nat. Genet.* 34, 287–291.
686 <https://doi.org/10.1038/ng1177>.

687 van Ruiten, M.S., and Rowland, B.D. (2021). On the choreography of genome folding: A
688 grand pas de deux of cohesin and CTCF. *Curr. Opin. Cell Biol.* 70, 84–90.
689 <https://doi.org/10.1016/j.ceb.2020.12.001>.

690 Samuelson, C., Radtke, S., Zhu, H., Llewellyn, M., Fields, E., Cook, S., Huang, M.-L.W.,
691 Jerome, K.R., Kiem, H.-P., and Humbert, O. (2021). Multiplex CRISPR/Cas9 genome editing
692 in hematopoietic stem cells for fetal hemoglobin reinduction generates chromosomal
693 translocations. *Mol. Ther. Methods Clin. Dev.* 23, 507–523.
694 <https://doi.org/10.1016/j.omtm.2021.10.008>.

695 Stevens, T.J., Lando, D., Basu, S., Atkinson, L.P., Cao, Y., Lee, S.F., Leeb, M., Wohlfahrt,
696 K.J., Boucher, W., O'Shaughnessy-Kirwan, A., et al. (2017). 3D structure of individual
697 mammalian genomes studied by single cell Hi-C. *Nature* 544, 59–64.
698 <https://doi.org/10.1038/nature21429>.

699 Sun, J.H., Zhou, L., Emerson, D.J., Phyo, S., Titus, K.R., Gong, W., Gilgenast, T.G.,
700 Beagan, J.A., Davidson, B.L., Tassone, F., et al. (2018). Disease-associated short tandem
701 repeats co-localize with chromatin domain boundaries. *Cell* 175, 224-238.e15.
702 <https://doi.org/10.1016/j.cell.2018.08.005>.

703 Szabo, Q., Jost, D., Chang, J.-M., Cattoni, D.I., Papadopoulos, G.L., Bonev, B., Sexton, T.,
704 Gurgo, J., Jacquier, C., Nollmann, M., et al. (2018). TADs are 3D structural units of higher-
705 order chromosome organization in *Drosophila*. *Sci. Adv.* 4, eaar8082.
706 <https://doi.org/10.1126/sciadv.aar8082>.

707 Szabo, Q., Donjon, A., Jerković, I., Papadopoulos, G.L., Cheutin, T., Bonev, B., Nora, E.P.,
708 Bruneau, B.G., Bantignies, F., and Cavalli, G. (2020). Regulation of single-cell genome
709 organization into TADs and chromatin nanodomains. *Nat. Genet.* 52, 1151–1157.
710 <https://doi.org/10.1038/s41588-020-00716-8>.

711 Tarjan, D.R., Flavahan, W.A., and Bernstein, B.E. (2019). Epigenome editing strategies for
712 the functional annotation of CTCF insulators. *Nat. Commun.* 10, 4258.
713 <https://doi.org/10.1038/s41467-019-12166-w>.

714 Ulianov, S.V., Velichko, A.K., Magnitov, M.D., Luzhin, A.V., Golov, A.K., Ovsyannikova, N.,
715 Kireev, I.I., Gavrikov, A.S., Mishin, A.S., Garaev, A.K., et al. (2021). Suppression of liquid–
716 liquid phase separation by 1,6-hexanediol partially compromises the 3D genome
717 organization in living cells. *Nucleic Acids Res.* 49, 10524–10541.
718 <https://doi.org/10.1093/nar/gkab249>.

719 Ushiki, A., Zhang, Y., Xiong, C., Zhao, J., Georgakopoulos-Soares, I., Kane, L., Jamieson,
720 K., Bamshad, M.J., Nickerson, D.A., University of Washington Center for Mendelian
721 Genomics, et al. (2021). Deletion of CTCF sites in the SHH locus alters enhancer-promoter
722 interactions and leads to acheiropodia. *Nat. Commun.* 12, 2282.
723 <https://doi.org/10.1038/s41467-021-22470-z>.

724 Vaillancourt, K., Yang, J., Chen, G.G., Yerko, V., Thérroux, J.-F., Aouabed, Z., Lopez, A.,
725 Thibeault, K.C., Calipari, E.S., Labonté, B., et al. (2021). Cocaine-related DNA methylation in
726 caudate neurons alters 3D chromatin structure of the IRXA gene cluster. *Mol. Psychiatry* 26,

727 3134–3151. <https://doi.org/10.1038/s41380-020-00909-x>.

728 Webster, D.E., Barajas, B., Bussat, R.T., Yan, K.J., Neela, P.H., Flockhart, R.J., Kovalski, J.,
729 Zehnder, A., and Khavari, P.A. (2014). Enhancer-targeted genome editing selectively blocks
730 innate resistance to oncokinase inhibition. *Genome Res.* *24*, 751–760.
731 <https://doi.org/10.1101/gr.166231.113>.

732 Willemin, A., Lopez-Delisle, L., Bolt, C.C., Gadolini, M.-L., Duboule, D., and Rodriguez-
733 Carballo, E. (2021). Induction of a chromatin boundary in vivo upon insertion of a TAD
734 border. *PLoS Genet.* *17*, e1009691. <https://doi.org/10.1371/journal.pgen.1009691>.

735 Winick-Ng, W., Kukalev, A., Harabula, I., Zea-Redondo, L., Szabó, D., Meijer, M., Serebreni,
736 L., Zhang, Y., Bianco, S., Chiariello, A.M., et al. (2021). Cell-type specialization is encoded
737 by specific chromatin topologies. *Nature* *599*, 684–691. [https://doi.org/10.1038/s41586-021-](https://doi.org/10.1038/s41586-021-04081-2)
738 [04081-2](https://doi.org/10.1038/s41586-021-04081-2).

739 Xu, Q., Chen, M., He, C., Sun, L., and Yuan, Y. (2013). Promoter polymorphisms in trefoil
740 factor 2 and trefoil factor 3 genes and susceptibility to gastric cancer and atrophic gastritis
741 among Chinese population. *Gene* *529*, 104–112. <https://doi.org/10.1016/j.gene.2013.07.070>.

742 Yang, Q., Jiang, N., Zou, H., Fan, X., Liu, T., Huang, X., Wanggou, S., and Li, X. (2022).
743 Alterations in 3D chromatin organization contribute to tumorigenesis of EGFR-amplified
744 glioblastoma. *Comput. Struct. Biotechnol. J.* *20*, 1967–1978.
745 <https://doi.org/10.1016/j.csbj.2022.04.007>.

746 Zhang, Y., Li, T., Preissl, S., Amaral, M.L., Grinstein, J.D., Farah, E.N., Destici, E., Qiu, Y.,
747 Hu, R., Lee, A.Y., et al. (2019). Transcriptionally active HERV-H retrotransposons demarcate
748 topologically associating domains in human pluripotent stem cells. *Nat. Genet.* *51*, 1380–
749 [1388](https://doi.org/10.1038/s41588-019-0479-7). <https://doi.org/10.1038/s41588-019-0479-7>.

750 Zhang, Y., Chen, F., and Creighton, C.J. (2021). SVExpress: identifying gene features
751 altered recurrently in expression with nearby structural variant breakpoints. *BMC*
752 *Bioinformatics* *22*, 135. <https://doi.org/10.1186/s12859-021-04072-0>.